International Journal of Design & Nature and Ecodynamics
Vol. 21, No. 6, June, 2026, pp. 1727-1737
Journal homepage: http://iieta.org/journals/ijdne

Effects of Fruit Maturity on Seed Traits, Germination, and ATR-FTIR-Based Seed Coat Chemistry of *Cymbidium finlaysonianum* Lindl. (Orchidaceae)

Popi Aprilianti[1,2], Surya Diantina[2], Ratna Yuniati[1], Dewi Pramanik[3], Elizabeth Handini[2], Dwi Murti Puspitaningtyas[2], Muhammad Idris[4], Retno Lestari[1*]

[1] Department of Biology, Faculty of Mathematics and Natural Sciences, Universitas Indonesia, Depok 16424, Indonesia
[2] Research Centre of Applied Botany, National Research and Innovation Agency, Cibinong 16911, Indonesia
[3] Research Centre of Horticulture, National Research and Innovation Agency, Cibinong 16911, Indonesia
[4] Department of Biology, Faculty of Mathematics and Natural Sciences, Universitas Andalas, Padang 25163, Indonesia

Corresponding Author Email: retno.lestari@sci.ui.ac.id

https://doi.org/10.18280/ijdne.210617

Received: 15 April 2026
Revised: 18 June 2026
Accepted: 25 June 2026
Available online: 30 June 2026

Keywords:
Attenuated Total Reflectance-Fourier Transform Infrared Spectroscopy, fruit maturity, lignin, orchid conservation, seed micromorphology

ABSTRACT

Cymbidium finlaysonianum is one of the fascinating Asian orchids. Understanding fruit, seeds, and their chemical components is essential for implementing conservation and commercial strategies. Lignin is one of the limiting factors in the germination process, which is present in the seed during fruit maturity. Thus, this study aims to observe the fruit morphology at different maturity stages and seed germination, to describe the seed morphology and morphometric characters, and to determine the chemical composition of *C. finlaysonianum* seeds. The fruit anatomy and seed micromorphology were analyzed by Field-Emission Scanning Electron Microscopy (FE-SEM). The in vitro germination of a few stages of the fruit was performed on Growmore® medium enriched with potato. The lignin and lipid components were examined using Fourier Transform Infrared Spectroscopy (FTIR). The results showed that fruit maturity can be detected in changes to the fruit skin (brownish-green with yellow seeds). The seed was categorised as very small with high seed air space (SAS) (97.93%). The seed was characterised by the presence of waxes and elevated anticlinal walls. There was no germination from the fruit 1 and 2 months after pollination (MAP), and the seeds from 3-5 MAP germinated with similar germination percentages. The chemical profile of the seed showed an increase in detectable lignin and lipid during seed maturation. These results provide valuable data on fruit maturity, seed morphology and chemistry, and germination, which are useful for conservation and commercial uses of the species.

1. INTRODUCTION

Orchidaceae is one of the most diverse families of plants. There are approximately 27.800 species in 880 genera that are dispersed in all of the continents except Antarctica [1]. The diversity of orchids includes their life forms, flowers, fruits, and seed morphology, as well as their vegetative parts [2]. *Cymbidium finlaysonianum* Lindl. is one of the orchid species that has beautiful yellowish-brown to dark reddish-brown flowers (Figure 1). Comber [3] stated that this species is common in South-East Asia but rare in Java, and that it occurs only in humid areas at 500 m above sea level. *Cymbidium finlaysoniamum* is popularly known as an ornamental plant with durable flowers (lasting 3 weeks) and a long inflorescence. Additionally, the flower comprises cyanidin-3-glycosides, an anthocyanin with antioxidant activity [4]. *Cymbidium finlaysonianum*, as a crassulacean acid metabolism plant, tends to have limitations in reproductive conditions for flowering and slow growth [5].

The orchid has dehiscent fruit, which relates to its adaptive strategies [2]. The seeds of orchids, known as dust seeds, have a specific shape, structure, and ornamentation of the seed coat, which consists of an embryo and an air space. This condition enables them to travel farther and reach remote areas [6, 7].

For commercial application, seeds from mature fruit are preferred because they can be stored for extended periods and transported efficiently [8]. Seed germination is fundamental for natural regeneration and the recovery of degraded populations [9]. However, seed germination is known to decline as the fruit matures. Few studies have directly compared the germination of immature and near-mature fruits of orchids, including *Cephalanthera falcata* [10], *Vanilla planifolia* [11], and *Ophrys* spp. [12], *Neuwiedia veratrifolia*, *Phalaenopsis aphrodite*, and *Cypripedium formosanum* [13]. These studies resulted in higher seed germination rates from near-mature seeds.

Lignin is known to be a limiting factor in seed germination in nature, persists in the seed coat, and is associated with fruit maturity [10, 13, 14]. On the contrary, lignin also protects the seed by imparting rigidity, which reduces water loss [15]. Seed from mature fruit has a higher lignin composition, which reduces the germination percentage [10]. Natural lignins

common in angiosperms are generally composed of p-hydroxyphenyl (H), guaiacyl (G), and syringyl (S) units. Meanwhile, C-lignin is found in limited taxa, such as Vanilla orchids and the genus *Melocactus* in the Cactaceae [16]. Since then, C-lignin has also been reported in the seed coats of Euphorbiaceae (*Jatropha*, *Ricinus*, and *Aleurites*) and *Cleoma hassleriana* (an ornamental plant, Cleomaceae) [17]. The latest study has revealed that the chemical composition of orchid seed coats can be analysed using Attenuated Total Reflectance (ATR)-Fourier Transform Infrared Spectroscopy (FTIR) [12, 13, 18]. The study of the chemical composition of orchid seeds has been conducted primarily in terrestrial species such as *Ophrys*, *Paphiopedilum*, *Neuwedia*, *Cypripedium*, and *Phalaenopsis*, as well as in epiphyte species [11-13, 18].

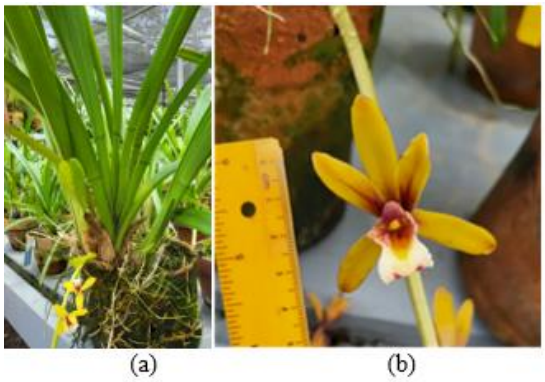

Figure 1. *Cymbidium finlaysonianum*: (A) the plant; (B) the flower

There is no report on fruit and seed characters, germination of a few maturity stages, and chemical composition of this tropical orchid, *C. finlaysonianum*. In the future, these characters can enhance our understanding of the ecological processes associated with dormancy, germination, and adaptation to specific habitats [6, 12, 19, 20]. These studies are also important for conservation and commercial purposes, including the use of immature fruit to maintain plant supply, as forest degradation and societal overexploitation threaten the existence of many orchid species. Thus, the study aims to observe the fruit at different maturity stages and their seeds in vitro germination, to describe the seed morphological characters, and to determine the chemical composition of the seeds of *C. finlaysonianum*. Nevertheless, this research was a preliminary study with a limited number of fruit samples (one per maturity stage).

2. MATERIALS AND METHODS

2.1 Plant material

The fruits of *C. finlaysonianum* were from the collection of Bogor Botanic Gardens, West Java. The plant was from East Kalimantan, and two individuals served as mother plants. The flowers from different plants were hand-pollinated in February 2024. The fruits for the immature and near-mature fruit study were harvested in the designated timeframe; they were 1, 2, 3, 4, and 5 months after pollination (MAP). Meanwhile, for seed characters, it used seeds from dehisced-mature fruit harvested at 6 MAP. The terminology of fruit maturity and the ages are shown in Table 1.

Table 1. Stage definition of fruit maturity

Fruit Age (Months after Pollination)	Maturity Stage
1	Immature
2	Immature
3	Near-mature
4	Near mature
5	Pre-cracking mature
6	Cracking mature

2.2 Fruit morphology

The observation of the fruit morphology used only one fruit for each fruit age, due to the limited number of fruits. This study was conducted on fruit harvested at 1, 2, 3, 4, and 5 MAP. After being picked, the fruit was measured and described, including the fruit size (length and diameter), weight, and the colour of the fruit and seed. The anatomical observation was conducted on 5 MAP fruits, since the fruits were determined to be pre-cracking mature, and this study was to confirm the parts of the mature fruit. The fruit was soaked in 96% alcohol for at least 7 days and cut at the target areas, namely the carpel margin and the centre, to observe the mid-section of the fruit.

The fruit anatomy was examined using Scanning Electron Microscopy (SEM) on an Aquilos 2 (Thermo Fisher Scientific), equipped with a field-emission gun at room temperature (±25 °C). Samples were transferred using a specialised cryogenic transfer system or a cooled cryo-holder. After entering the vacuum chamber, the samples were mounted on an actively cooled cryo-stage and coated with a thin layer of platinum (~5 nm thickness) using a sputter coater. The imaging was achieved with an accelerating voltage of 4 kV, a beam current of 25 pA, and working distances of 9-16 mm. The samples were then ready to be recorded.

2.3 In vitro seed germination

The seeds of *C. finlaysonianum* were germinated in vitro. The medium used was Growmore® fertiliser (for the vegetative phase, NPK 32:10:10) (2 g L^{-1}) as the main active component, with the addition of potatoes (15 g L^{-1}), peptone (2 g L^{-1}), sugar (30 g L^{-1}), and active charcoal (1 g L^{-1}), named the Growmore-based supplemented (GS) medium. The potato skin was peeled, weighed, and crushed in a blender with peptone and sugar. The solution pH was fixed at 5.6 ± 0.1, then solidified using 7 g L^{-1} agar. The flask size was 330 mL with 50 mL of medium. The medium was then autoclaved for 25 minutes at 121 °C.

The germination experiment used a completely randomised design with one factor, fruit maturity age (1, 2, 3, 4, and 5 MAP). The GS medium was plated in four Petri dishes (60 × 15 mm), each containing 30 mL of medium. Due to limited fruit availability, this study used only one fruit per stage, and the Petri dishes were treated as experimental units for germination screening rather than true biological replicates. Then, there were 4 experimental units for each fruit stage.

The sterilisation process began with washing the fruit with dishwashing liquid, rinsing it under running water, and allowing it to air-dry. The process continued in a UV-sterilised, laminar airflow cabinet. Fruit was immersed in 96% alcohol and flamed with a Bunsen burner. This process was repeated three times. Subsequently, the fruits were placed in sterile Petri dishes and cut at both ends and in the middle. The central portion was opened. Since the seed of the orchid was a

dust seed with a very minute size, the seeds were distributed evenly onto the germination medium.

Seed cultures were incubated at room temperature (approximately 25 ℃) under a 16-hour photoperiod with a light intensity of 2222.67 lux. Seeds that developed protocorms were considered germinated and were recorded two months after sowing. Germination was assessed using a light microscope (Olympus U-TV0.5XC-35 H 12344 JAPAN) and counted for ±100 seeds for each replication. The germination percentage was then calculated by using the formula:

$$Germination\ percentage = \frac{Germinated\ seeds}{Total\ number\ of\ seeds} \times 100\%$$

2.4 Seed characters

The observation of seed characters used seeds from dehiscent fruit (6 MAP fruit). The seeds were desiccated for 3-7 days. First, the seeds were sterilised with chlorox solution (5%) for 2 minutes and rinsed with sterile distilled water, to facilitate the clear measurement of the seeds [21]. A total of 40 seeds were observed under an Olympus BX-43 light microscope [22] to measure seed length (SL) and width (SW), and the embryo length (EL) and width (EW). From those measures, other morphological parameters were calculated, i.e., seed volume (SV), embryo volume (EV), SV/EV, and seed air space (SAS). The SV (× 10^{-3} mm^3), EV (× 10^{-3} mm^3), and SAS (%) were calculated with the following formula [6]:

$$Seed\ Volume = 2[(\mathrm{SL}/2)(\mathrm{SW}/2)^2(\pi/3)$$

$$Embryo\ Volume = 4/3\pi(\mathrm{EL}/2)(\mathrm{EW}/2)^2$$

$$Seed\ Air\ Space = ((\mathrm{SV}-\mathrm{EV})/\mathrm{SV})\mathrm{x}100\%$$

The seed surface was observed using an SEM JSM-IT 200. The seed samples were sputter-coated with gold before SEM observation. The observation included the whole seed, the mid-region, the chalazal, and the micropylar region [21]. The SEM results were used to identify the qualitative characteristics, i.e., seed shape, anticlinal and periclinal wall structure, and cell shape [22].

2.5 Fourier Transform Infrared Spectroscopy analysis

The chemical analysis of the seeds was performed using ATR-FTIR equipped with a UATR unit cell from PerkinElmer (PerkinElmer Corporation, Waltham, MA, USA). The experiment used the fruits of *C. finlaysonianum*, harvested at 1, 2, 3, 4, and 5 MAP, with one fruit per maturity age. To obtain the samples for analysis, the fruit was cut, the seeds were placed in a Petri dish, and the water content was reduced by storing the seeds in a desiccator for 7 days. The chemical content was then analysed using an FTIR spectrometer, as described by research [12]. This analysis used only one replicate for each maturity age fruit.

Seeds were analysed without any prior processing and were placed on an ATR crystal plate, which pressed the sample to facilitate direct interaction between the instrument's light, the seed sample, and the reflected radiation detected by the spectrometer. Infrared radiation was applied over the 4000-400 cm^{-1} range at 25 ℃. The sample spectra were acquired from 16 scans per sample at a resolution of 4 cm^{-1} and a data interval of 1 cm^{-1}. The FTIR analysis results were displayed as spectra, or graphs of transmittance percentage versus frequency. The peak frequencies were determined using PerkinElmer Spectrum Two FTIR-UATR.

Spectral data processing was performed using PerkinElmer Spectrum 10 software. Automatic baseline correction was applied to all raw spectra to eliminate background distortions caused by crystal contact and light scattering. Spectral smoothing was then performed in the software using the Savitzky-Golay algorithm to increase the signal-to-noise ratio and remove high-frequency digital noise. Subsequently, Min-Max normalisation was conducted to standardise the Y-axis intensity (percent transmittance; %T), allowing for an accurate and objective comparison between the samples [12, 13].

For analysing the spectra, we separated the functional group region (4000-1500 cm^{-1}) and fingerprint region (1500-400 cm^{-1}), then identified the major peaks in 4000-2500 cm^{-1}, 2500-2000 cm^{-1}, and 2000-1500 cm^{-1} zones. The peak characteristics were then evaluated based on their intensity (strong, medium, weak) and shape (rounded or sharp). Band variations may occur, and some chemical components may exhibit different bands. We prioritised bands that are clearly visible and well-interpretable, and focused on the assessment of the spectra presented in the following, which can reveal the chemistry of the seed [12].

2.6 Data analysis

Fruit morphology was analysed qualitatively and described using the terminology of research [2], while seed morphology was described according to studies [6, 7]. The distribution map of *C. finlaysonianum* was created using ArcGIS Earth version 2.7.1, with species occurrence data from the Global Biodiversity Information Facility (GBIF) [23]. Seed germination was presented descriptively. The FTIR results for chemical contents in the seed coat were presented as spectra, with each band showing chemical differences across fruit ages. The chemical composition was determined based on previously published methods [12, 13, 24-28].

3. RESULTS AND DISCUSSION

3.1 Fruit morphology

Cymbidium finlaysonianum has a large fruit size, about 4 cm in length and 1.5 cm in diameter at 1 MAP, and increases in size and weight during maturity (Table 2). In this study, fruit length and diameter increased greatly from 1–4 MAP, particularly at the first and fourth MAP, but slowed from 5 MAP onward. These 1–3 MAP fruits increased in weight slowly; then the 4 MAP fruit weighed twice as much as the 3 MAP fruit, even though the size of those fruits was not that different. It demonstrates that fruit development had almost finished, and cell enlargement increased significantly in the fertile valve areas [2].

This growth was also accompanied by a change in the fruit skin colour from dark green to brownish green. In this condition, the fruit skin was still hard and rigid. When the size increment slowed at 4 MAP, and the fruit skin at 5 MAP started to soften, the fruit dehisced at 6 MAP. Research [29] supported this result, that the mature seed capsule has softer skin with red-brown colouration.

Table 2. The characters of the fruit and seed of *Cymbidium finlaysonianum* at different fruit maturity stages

Fruit Age (Months after Pollination)	Fruit Length (cm)	Fruit Diameter (cm)	Weight (g)	Skin Fruit Color	Seed Relative Humidity (%)	Seed Color
1	4	1.5	10.3	Green	No data	Milky white
2	5.5	2.5	13.74	Green	79	Milky white
3	6	2.7	15.01	Dark green	78	Yellowish-white
4	7	3.2	31.11	Brownish-green	62	Yellowish-white
5	7.2	3.5	40.63	Brownish-green	60	Yellow

Note: Measurements were obtained from a single representative fruit per stage; values represent single measurements.

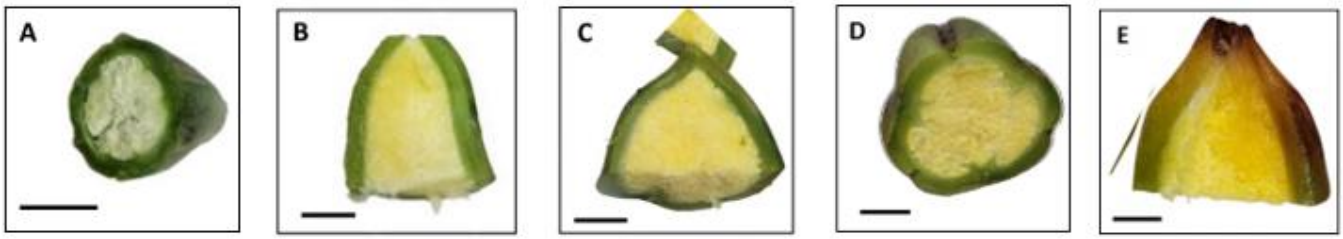

Figure 2. Morphology of the seed development of *Cymbidium finlaysonianum*. (A) Milky white seeds at 1 MAP, (B) milky white seeds at 2 MAP, (C) fusiform and clump seeds at 3 MAP, (D) fusiform and clump seeds at 4 MAP, (E) fusiform seeds at 5 MAP
Notes: Scale bars: 1 cm. MAP: Months after pollination.

Table 2 and Figure 2 also show the conditions inside the fruit; the 1 and 2 MAP fruits had seeds with similar colour and shape, milky white, filiform, and densely packed, filling the fruit space (Figure 2(A-B)). The seed had nearly colourless testa, in contrast with the 3 and 4 MAP seeds that appeared as filament clumps, and their colour changed to yellowish-white, with a clear testa pattern (Figure 2(C-D)).

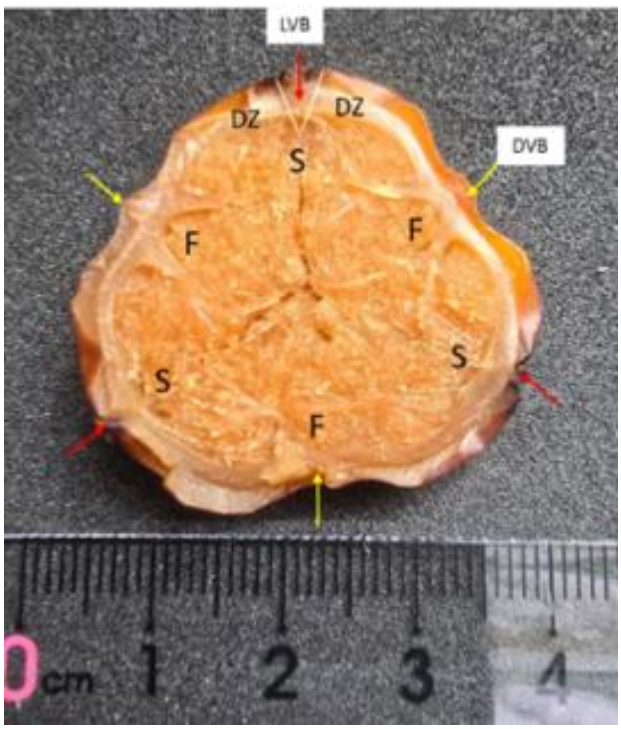

Figure 3. The fruit cross-section of *Cymbidium finlaysonianum* at 5 MAP
Notes: DZ: Dehiscence zone (white line), F: Fertile valve, yellow arrow; S: Sterile valve, red arrow; LVB: Lateral vascular bundle; DVB: Dorsal vascular bundle. MAP: Months after pollination.

Along with the final development of the fruit, the seeds began to disperse within it, and the colour turned yellow until they started to mature at 5 MAP (Figure 2(E)). The changes in fruit skin colour were in line with seed colour. Thus, this colour shift of fruit skin can indicate when the fruit can be harvested to produce seeds with high viability, especially since the species' seed viability declined after 2 years of storage and was completely lost after 6 years [30].

Figure 3 shows the whole fruit cross-section of the near-mature 5 MAP fruit of *C. finlaysonianum*. It shows that they have six valves, divided into three fertile valves (yellow arrow) and three sterile valves. The parenchymal cells in the sterile and fertile valve areas have a compact, rectangular shape. In the centre of each valve, there is a vascular bundle, either dorsal (Figure 3, Figure 4(A)-white circle, Figure 4(B)) or lateral (Figure 3, Figure 4(C)-blue circle, Figure 4(D)). The differences between these two types of valves are that the cells of fertile valves originated from carpels and will expand during fruit maturation (Figure 4(B)), while the sterile valves originated from sepals and will remain at a constant size (Figure 4(D)) until the fruit matures [2, 31].

The sterile and fertile valves are separated by the dehiscent zone, characterised by small single-layered cells (Figure 3, Figure 5(A)-yellow line), which lignify at the innermost endocarp cell layer at a later phase of fruit maturation [2]. The V-shape of the dehiscence zone is usually shown in late development. The endocarp of this fruit consists of a single layer with small, rectangular, thin-walled cells (Figure 5(B)-red arrow). Also, trichomes formed in this area (Figure 5(B)-yellow arrow), thickened, and lignified.

Other findings show that the skin of the fruit of *C. finlaysonianum* has a thick layer of cells (exocarp) that protects the fruit from ultraviolet light under the tree canopy and helps minimise desiccation, thereby maintaining humidity inside the fruit. This thick exocarp is also one of the distinguishing features between epiphyte and terrestrial orchid fruit, since the latter has a thinner-walled fruit [2].

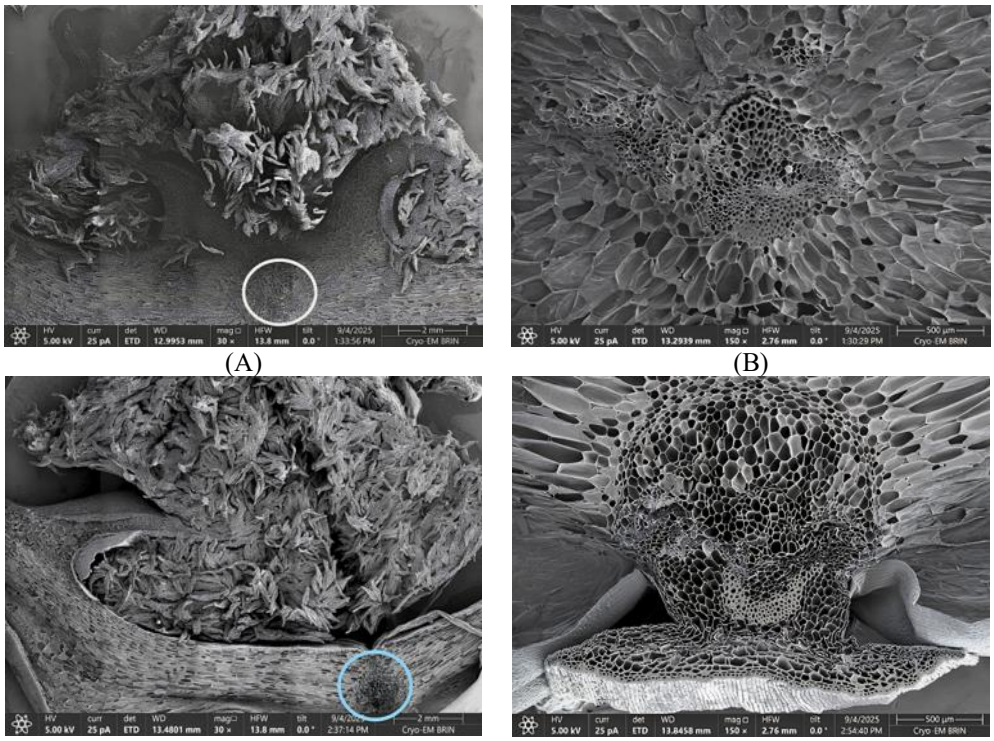

Figure 4. Fruit cross-section from Cryo-Field-Emission Scanning Electron Microscopy (FE-SEM) of *Cymbidium finlaysonianum* at 4 MAP (A) fertile valve of the fruit, dorsal vascular bundle (white circle), (B) the cells of the dorsal vascular bundle, (C) sterile valve of the fruit, lateral vascular bundle (blue circle), (D) the cells of the lateral vascular bundle
Notes: Scale bars: A-C 2 mm, B-D 500 µm

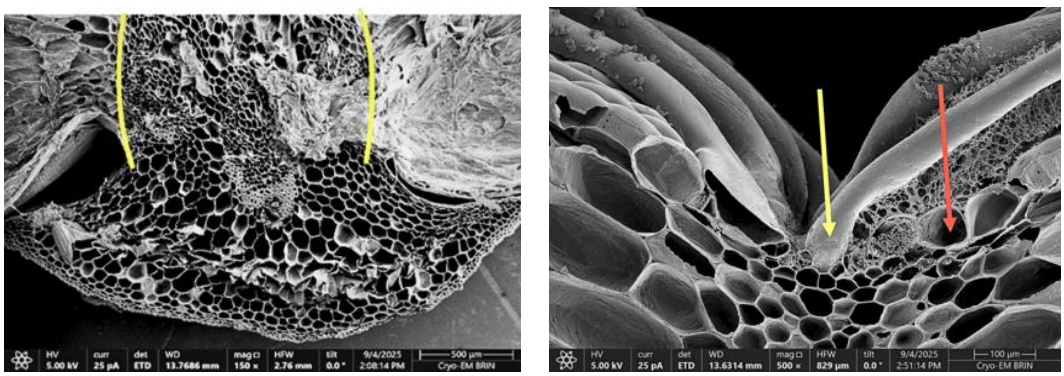

Figure 5. (A) The dehiscence zone (yellow line) and (B) the endocarpic trichome (yellow arrow) and endocarp layer (red arrow) in the sterile valve area of 4 MAP fruit of *C. finlaysonianum*
Notes: Scale bars: (A) 500 µm, (B) 100 µm.

3.2 Seed characters

The orchid fruit has a million dust seeds, which are generally dispersed by the wind [6]. This seed has a simple structure: an undifferentiated globular embryo, wrapped in a single layer of the seed coat. When the globular embryo has formed, seed development stops and continues as the seed elongates until it matures [32, 33]. C*ymbidium finlaysonianum* has a minute, yellow, mature seed with a fusiform shape (Figure 6(A-B)). Based on the measurement results (Table 3), the seed was classified as a very small seed (0.1-0.2 mm) according to research [6], specifically as a cymbidium-type seed. The embryo was located in the middle of the seed (Figure 6(A)), with a tiny size: 0.029 mm in length and 0.014 mm in width (Figure 6(A) and Table 3). The seed's SL/SW ratio is 3.24, indicating the seed was truncated (SL/SW < 6).

From our study, the seed characters of *C. finlaysonianum* support the main characters of epiphyte orchids, including rectangular testa cell walls and parallel orientation to the axis in the median part (Figure 6(C)) of the seed. Meanwhile, the chalazal pole tended to be rounded (Figure 6(D)), and the micropylar area had the same shape but smaller testa cells (Figure 6(E)). This shape also occurs in *Phalaenopsis* species [34], and the seed's surface was velvety, indicating the presence of waxes that protect the embryo by creating a hydrophobic condition during dispersal and are adaptive in the new habitat [19]. The micromorphology of the seeds recorded that the seed testa had a longitudinal line of periclinal wall ornamentation (Figure 6(C)-yellow arrow). The testa cell also shows the arch of the anticlinal walls (Figure 6(B)-red arrow).

This cell also appeared raised and thickened. These elevated anticlinal walls are also a common characteristic of the

subfamily Epidendroideae, which may slow the seeds' descent through the air, thereby allowing them to attach to the substrate properly in nature [7, 19]. This result is also supported by the high SAS of the species (97.93%) and the high ratio of seed volume to embryo volume in this study (56.73%), indicating a light, buoyant seed, which may allow the seed to disperse in a broader geographical area [20, 21, 33-36].

The global biodiversity information facility (GBIF) records for *C. finlaysonianum* showed that its distribution covered a large area, including Cambodia, Vietnam, Thailand, Myanmar, the Philippines, Malaysia, Sumatra, Java, Borneo, Sulawesi, and the Moluccas (Figure 7), at altitudes ranging from sea level to 500 m. In the present study, seed buoyancy suggests a direct link to the species' distribution area. Meanwhile, buoyancy in the seeds resulted from the large portion of SAS caused by the increase in testa cell length [33, 36].

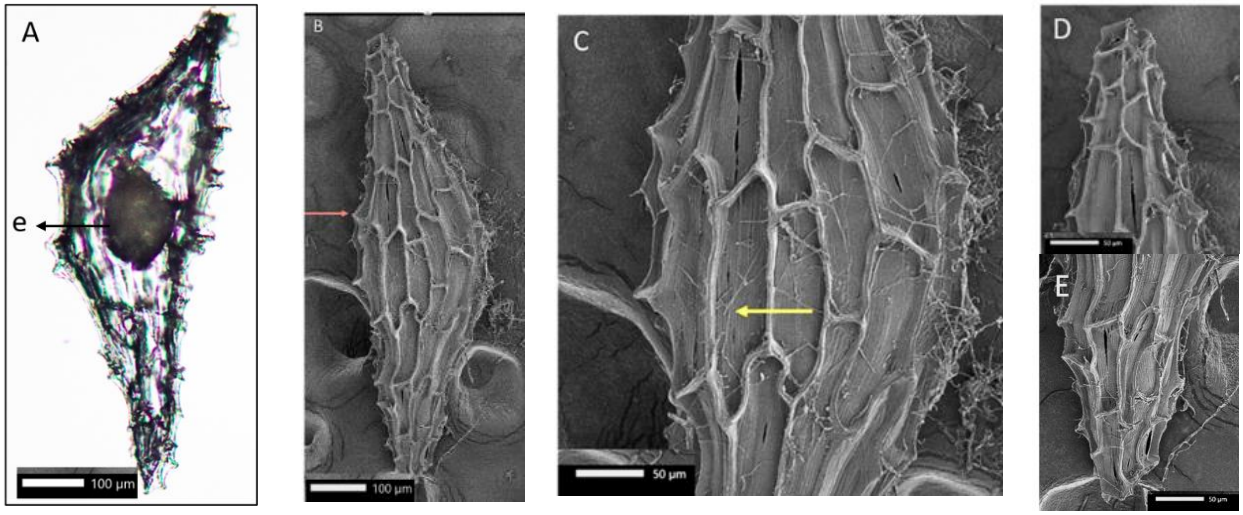

Figure 6. The seed of *Cymbidium finlaysonianum* (A) full seed from light microscope (e - embryo), (B) full seed from Scanning Electron Microscopy (SEM) (red arrow shows the arch of the anticlinal walls), (C) the medial part of the seed (yellow arrow indicates the ornamentation of the periclinal walls), (D) The cells of the chalazal pole; (E) the cells of the micropylar pole
Notes: Scale bars: A-B: 100 µm, C-E: 50 µm.

Table 3. The seed morphometry and morphology of *Cymbidium finlaysonianum*

SL (mm)	SW (mm)	SL/SW	SV (mm^3)	EL (mm)	EW (mm)	EL/EW	EV (mm^3)	SV/EV	SAS (%)
0.184 ± 0.01	0.058 ± 0.009	3.24 ± 0.61	$16.2 \times 10^{-5} \pm 4.1 \times 10^{-5}$	0.029 ± 0.003	0.014 ± 0.002	2.02 ± 0.31	$3.1 \times 10^{-6} \pm 10^{-6}$	56.73 ± 29.15	97.93 ± 0.86
Seed shape	Embryo location	Periclinal wall ornamentation		Testa cell shape differences*	Testa cell shape of the median area		Orientation of testa cells	Anticlinal wall	Waxes
Fusiform	Centre of the axis	Longitudinal line		Present	Rectangular		Parallel	Raised and thickened	Present

Note: *Testa cell shape differences in the median, micropylar, and chalazal area. SL: seed length, SW: seed width, SV: seed volume, EL: embryo length, EW: embryo width, EV: embryo volume, SAS: seed air space.

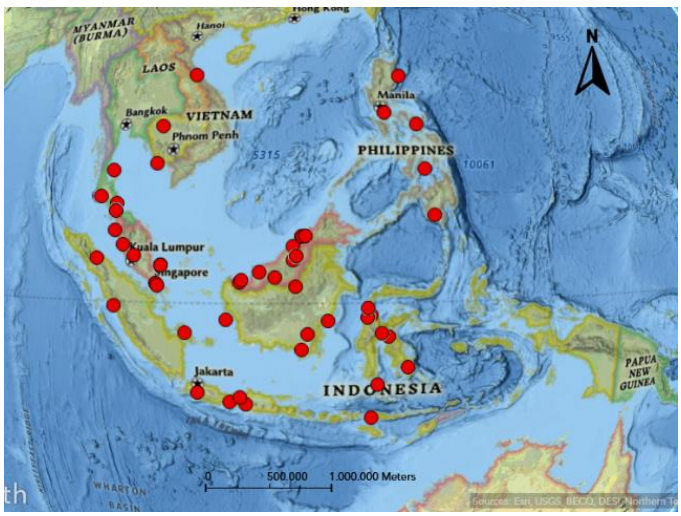

Figure 7. The distribution area of *Cymbidium finlaysonianum*

Source: GBIF species occurrence data.

3.3 Seed germination

Seeds for the germination study originated from a single fruit at each maturity age, due to limited fruit availability per stage; therefore, the results were interpreted as preliminary and require validation with additional fruits. The germination percentages are then described in terms of descriptive trends. It showed that the various maturity stages of *C. finlaysonianum* fruit correlated with seed physiological maturity, as evidenced by successful germination at 12 weeks of incubation at room temperature. Seed germination was not observed in seeds harvested at 1 or 2 MAP (Figure 8), indicating that immature seeds were not adequate to support the germination process. Furthermore, 70% germination was observed in seeds harvested at 3, 4, and 5 MAP (Figure 8), suggesting embryo development and maturity that support germination.

The 1-2 MAP fruits had nearly colourless testa, and this condition persisted for 12 weeks of observation after sowing

in the germination medium (Figure 9(A-B)). There were no changes or germination during incubation at room temperature. Meanwhile, the seeds of 3 and 4 MAP started to germinate at 6 weeks after sowing (WAS) (Figure 9(C-D)), with high germination percentages (70%), whereas 5 MAP fruit had slightly lower germination, with no significant difference.

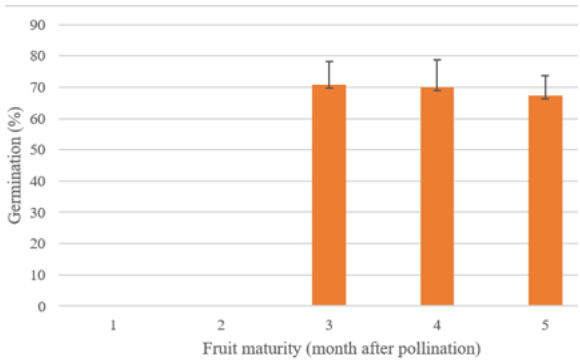

Figure 8. Seed germination of *Cymbidium finlaysonianum* from several fruit maturity ages

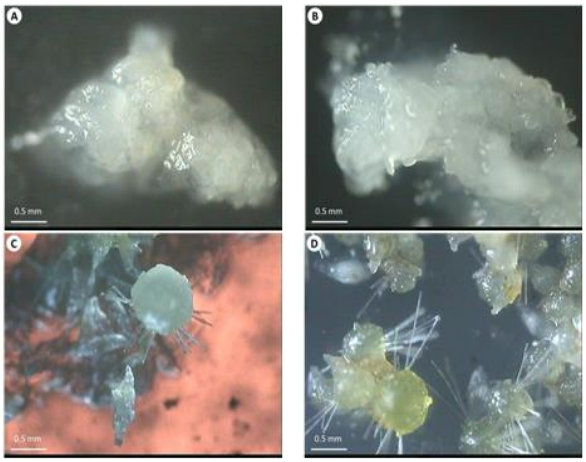

Figure 9. In vitro seed germination of *Cymbidium finlaysonianum* on Growmore-based supplemented (GS) medium 3 months after sowing, using seeds from fruits harvested at different maturity stages. (A) 1 month after pollination (MAP), (B) 2 MAP, (C) 3 MAP, (D) 4 MAP

Notes: MAP: Months after pollination.

This result revealed that colourless seeds will not germinate, whereas the near-mature fruit with yellow seeds germinates at a high percentage. The difference between seeds from two fruit conditions was supported by research [29], which grouped immature and near-mature seeds of orchid species from Madagascar, including *Angraecum* spp., which have a clear testa, in contrast to dark-brown mature seeds. In this study, we classified white seeds as immature and yellowish seeds as near-mature. This result can serve as an indicator for in vitro propagation using yellowish to yellow seeds (3-5 MAP fruits) to produce more plants for the ornamental plant industry supply. The colourless testa or white appearance of the seed in the immature fruit is related to the lignification of the seed [37]. The decrease in germination rate can be attributed to near-mature seed fruit beginning to produce lignin, which creates a hydrophobic environment that restricts water and nutrient absorption [38].

3.4 Fourier Transform Infrared Spectroscopy analysis

The characterisation of functional groups in the seed *of C. finlaysonianum* across different fruit maturity ages (1, 2, 3, 4, and 5 MAP) was evaluated using FTIR to elucidate the biochemical dynamics during fruit development, as shown in Figure 10 and Table 4. The orchid seed consists of biochemical materials such as cellulose, lignin, lipids, and proteins. These compounds were detected with infrared spectra. The spectra were shown as relative peak intensity, and the quantitative comparison of component concentrations was not performed; the observed changes in %T represent relative changes in spectral absorbance.

This study highlights the lignin and lipid components of the seed to confirm the form of lignin and lipid during seed maturation. Along with seed development, lipids and lignin were deposited. Research [13] stated that differences between the near-mature and mature stages are relatively small and are largely characterised by lipid and lignin accumulation. As we know, Orchidaceae, or plants in general, possess the G and S types of lignin, with a low level of H units [16]; meanwhile, the C unit is a rare type of lignin that is found in transgenic plants [39].

Table 4. The band position of lipid and lignin of *Cymbidium finlaysonianum* fruit at several ages of maturity based on ATR-FTIR results

Component	Wavenumber of Seed Coat Composition During Fruit Maturity (MAP) (cm^{-1})					Functional Groups/ Chemical Assignment
	1	2	3	4	5	
Cellulose and lignin	3331	3292	3275	3328	3289	O-H stretching vibrations (hydrogen-bonded) [12]
Lipids	2917	2917	2917	2917	2916	Methylene C-H Asymmetric Stretching vibrations [12, 13, 25, 26]
Lipids	2850	2849	2849	2849	2849	Methylene C-H Symmetric Stretching vibrations [12, 13, 26]
Hemicellulose	1737	1733	-	1733	1735	C = O stretching vibration of carboxyl and acetyl group [12]
G/S-lignin/C-lignin	-	1606	-	-	-	C = C aromatic ring stretching vibration of lignin [12, 13, 25-27]
C-lignin	-	-	1593	1595	1599	C = C-C aromatic skeletal stretching vibration of lignin [12, 13, 25, 26]
G/S-lignin	1514	1513	1514	1514	1512	Aromatic ring stretch + in-plane C-H bending (ν(Ar) + δAr-H) [13]
C-lignin	-	-	-	1316	1311	C-O Carbonyl [13, 28]
Cellulose	1017	1013	1045	1032	1030	C-O Carbonyl [28]

Notes: MAP: Months after pollination.

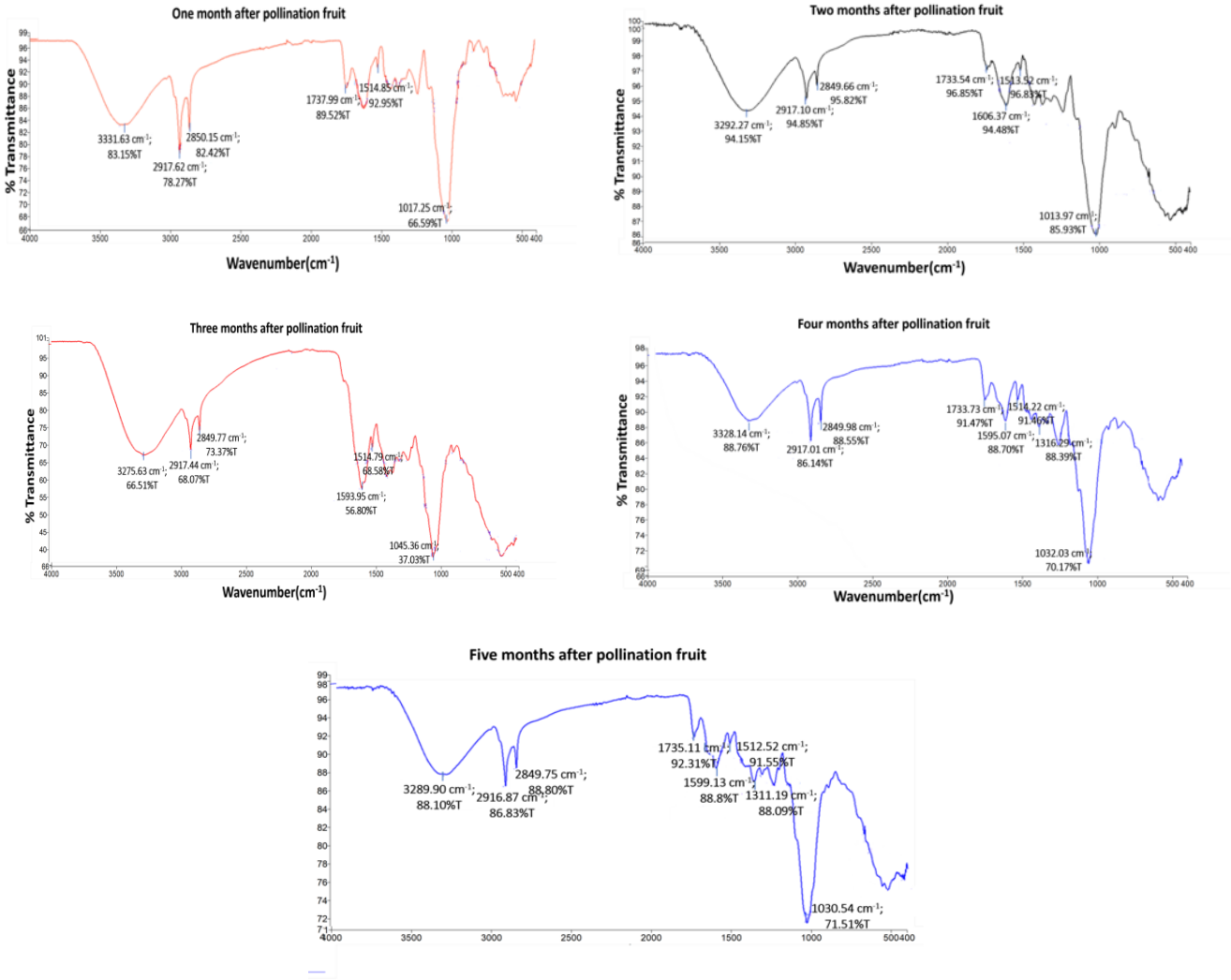

Figure 10. Fourier Transform Infrared Spectroscopy (FTIR) spectra of *Cymbidium finlaysonianum* seed at 5 ages of fruit maturity

The FTIR spectrum exhibits a broad peak at 3328/3329 cm^{-1}, which was assigned to cellulose, a common constituent of plant species [12]. Also, it detected the presence of lipid components at the beginning of fruit development, which were confirmed by the appearance of sharp and intense doublet peaks between 2916 and 2850 cm^{-1}, representing the asymmetric and symmetric C-H stretching vibrations of aliphatic chains, respectively (Figure 10 and Table 4). Temporally, lipid density reaches its maximum accumulation at 3 MAP, serving as a critical biochemical index of physiological maturity.

The FTIR spectra also showed that G/S-lignin (1514-1512 cm^{-1}) was formed at the earliest seed stage, and its deposition remained stable through the later stages (Table 4 and Figure 10). A similar result was also found in the seed coat of the orchids *Phalaenopsis* and *Cypripedium* [12]. Moreover, the G/S-lignin, which was shown as different bands (1512, 1513, and 1514 cm^{-1}), exhibits the heterogeneity of this lignin type. The observed variation in lignin-associated bands in the fingerprint region may be attributed to developmental changes in lignin composition and cell wall architecture during fruit maturation, in agreement with an earlier study [13] on *Phalaenopsis*, *Cypripedium*, and *Neuwiedia* species. Also, the peak size of this lignin showed dynamic trends across maturity stages. It initiates at the relative peak intensity of 85.94 (1 MAP), expands dramatically to its maximum size at 56.80 (3 MAP), and subsequently relaxes to a stabilised plateau of relative peak intensity at 88.82 during the late stages (4 and 5 MAP). According to research [13], this distinct fluctuation in peak size reveals that G/S-lignin is deposited early in seed development to build the foundational cell wall framework. The subsequent reduction in peak size at 4-5 MAP does not imply polymer degradation but rather reflects a structural embedding effect, in which the consolidation of the newly synthesised, highly linear catechol-lignin (C-lignin) matrix encapsulates the pre-existing G/S-lignin network.

Furthermore, the C-lignin (1593 cm^{-1}), which derives from caffeyl alcohol, began to be synthesised in the later stage (3 MAP), and it broadened at the last stage (1599-1595 cm^{-1}) (Figure 10 and Table 3). The prominent absorption band at 1593 cm^{-1} is assigned to the symmetric aromatic skeletal stretching vibration (C-C bonds in aryl rings). Notably, while G/S-lignin strongly influences the 1514 cm^{-1} region, the catechyl ring structures of catechyl-lignin (C-lignin) express a highly enhanced signal at 1593 cm^{-1} due to the symmetrical nature of its linear benzodioxane linkage. It reached a maximum thickness of 56.80%T at 3 MAP, before stabilising at ~88.80%T at 4 and 5 MAP. The maximum peak at 3 MAP serves as a decisive biochemical marker of the completion of seed coat lignification. The successful polymerisation of the

linear C-lignin shield provides a structural maturity process to the seed, which biologically validates the dramatic breakthrough in germination success, shifting from 0% in immature stages to an optimal, sustained baseline of ±70% from 3 MAP onwards [11, 13, 16, 40]. This C-lignin was also detected in *Vanilla planifolia* during fruit maturity [40]. A study [41] on *Cleoma hassleriana* found that during seed maturation, G and C-lignins were differentially deposited and regulated, with C-lignin forming sequentially after G-lignin within the same testa layer.

The lipid bands at 2917 and 2850 cm^{-1} and G/S-lignin/C-lignin at 1606 cm^{-1} are also found in the seed coat of *Ophrys* spp., *Neuwiedia veratrifolia*, and *Cypripedium formosanum*. However, *Ophrys* spp. showed no C-lignin (1593, 1595, 1599 cm^{-1}) or G/S-lignin (1512, 1513, and 1514 cm^{-1}) in references [12, 13]. Because *Ophrys*, *Neuwiedia*, and *Cypripedium* are terrestrial species, C-lignin appears to occur inconsistently. This suggests that C-lignin may be evolutionarily flexible rather than deeply conserved. C-lignin has a relatively uniform, acid-resistant structure, which may provide structural rigidity and protect the seed. Meanwhile, lipids, including cutin, suberin, and wax, form hydrophobic barriers that reduce water permeability in seed coats. In suitable habitats, these lipids help regulate seed dormancy and germination. Together, lignin and lipids form an effective double-layer defence in the seed coat [13]. The lack of difference in germination results for 3-5 MAP might be due to near-mature seeds not yet having reached the hydrophobic state [29].

C-lignin probably did not affect seed pigmentation. This was supported by research [13], which stated that there is no strong association between C-lignin and pigmentation in the seed coat. The presence of polyphenols and flavonoids is responsible for this pigmentation on the orchid seed coat [42]. Still, the presence of C-lignin may be linked to pigmentation dynamics through concurrent changes in tannin and fatty acid composition during maturation [12].

4. CONCLUSIONS

Studying the fruit, seed, and seed chemical composition of *C. finlaysonianum* provided new insights into the species, including for conservation and commercial purposes. Understanding the immature and mature processes can provide a practical method for propagating plants to increase plant supply. This study provides useful information on harvesting fruit at 3-5 MAP to obtain more germinated seeds. Investigating the seed characters of *C. finlaysonianum* confirms morphological traits associated with its epiphytic life form. The chemical profiles obtained by FTIR are aligned with seed functionality and viability. The accumulation of lipid and C-lignin may be linked to the maturation process; in contrast, both lignin and lipid serve protective functions for the seed during maturation, dispersal, and germination. Further study is required to determine how seed maturity relates to seed coat lignification.

ACKNOWLEDGMENT

This work was supported by the Research Organisation for Life Sciences and Environment, the National Research and Innovation Agency, which provided funding for the Rumah Program, and the Directorate of Scientific Collection Management (Bogor Botanic Gardens), which supported the use of the orchid collection. The authors also acknowledge the facilities and scientific and technical support from Cryo EM Laboratories-Aquilos2, the National Research and Innovation Agency through E-Layanan Sains, Badan Riset dan Inovasi Nasional. All of the authors are main contributors and contributed equally throughout the research and publication process.

REFERENCES

[1] Givnish, T.J., Spalink, D., Ames, M., Lyon, S.P., et al. (2016). Orchid historical biogeography, diversification, Antarctica and the paradox of orchid dispersal. Journal of Biogeography, 43(10): 1905-1916. https://doi.org/10.1111/jbi.12854

[2] Dirks-Mulder, A., Ahmed, I., uit het Broek, M., Krol, L., et al. (2019). Morphological and molecular characterizations of orchid fruit development. Frontiers in Plant Science, 10: 137. https://doi.org/10.3389/fpls.2019.00137

[3] Comber, J.B. (1990). Orchids of Java. Kew, Bentham-Moxon Trust. https://archive.org/details/orchidsofjava0000comb/page/n7/mode/2up.

[4] Teoh, E.S. (2016). Medicinal Orchids of Asia. Springer Cham. https://doi.org/10.1007/978-3-319-24274-3

[5] Nahar, S.J., Haque, S.M., Kazuhiko, S. (2015). Organogenesis of *Cymbidium finlaysonianum* under different sources of light. American-Eurasian Journal of Agricultural & Environmental Sciences, 15(10): 2095-2102.

[6] Arditti, J., Ghani, A.K.A. (2000). Numerical and physical properties of orchid seeds and their biological implications. New Phytologist, 145: 367-421. https://doi.org/10.1046/j.1469-8137.2000.00587.x

[7] Barthlott, W., Große-Veldmann, B., Korotkova, N. (2014). Orchid Seed Diversity: A Scanning Electron Microscopy Survey. Botanischer Garten und Botanisches Museum Berlin-Dahlem.

[8] Kitsaki, C.K., Zygouraki, S., Ziobora, M., Kitzios, S. (2004). In vitro germination, protocorm formation and plantlet development of mature versus immature seed from several Ophrys species (Orchidaceae). Plant Cell Reports, 23: 284-290. https://doi.org/10.1007/s00299-004-0841-8

[9] Ekasari, I., Lailati, M., Nurlaeni, Y., Puspanti, A., Mufida, Y.R. (2025). Seed morphology and seedling growth modelling for Litsea cordata and Sloanea sigun in Java Montane Forests. International Journal of Design & Nature and Ecodynamics, 20(3): 547-554. https://doi.org/10.18280/ijdne.200310

[10] Yamazaki, J., Miyoshi, K. (2006). In vitro asymbiotic germination of immature seed and formation of protocorm by Cephalanthera falcata (Orchidaceae). Annals of Botany, 98: 1197-1206. https://doi.org/10.1093/aob/mcl223

[11] Yeh, C.H., Chen, K.Y., Lee, Y.I. (2021). Asymbiotic germination of Vanilla planifolia in relation to the timing of seed collection and seed pretreatments. Botanical Studies, 62: 6. https://doi.org/10.1186/s40529-021-00311-y

[12] Aytar, E.C., Deniz, I.G., Incedere, D., Kompe, Y.O.,

Basili, T., Harzli, I., Durmaz, A. (2024). Comparison of seed morphology and seed coat chemistry in Ophrys (Orchidaceae) species. ACS Omega, 9: 33773-33788. https://doi.org/10.1021/acsomega.4c03130
[13] Barsberg, S.T., Lee, Y.I., Rasmussen, H.N. (2018). Development of C-lignin with G/S-lignin and lipids in orchid seed coats-an unexpected diversity exposed by ATR-FT-IR spectroscopy. Seed Science Research, 28(1): 41-51. https://doi.org/10.1017/S0960258517000344
[14] Liang, M.X., Davis, E., Gardner, D., Cai, X.N., Wu, Y.J. (2006). Involvement of AtLAC15 in lignin synthesis in seeds and in root elongation of Arabidopsis. Planta, 224: 1185-1196. https://doi.org/10.1007/s00425-006-0300-6
[15] Shah, T.A., Li, Z.H., Li, Z.Y., Z, A.D. (2022). Composition and role of lignin in biochemicals. In Lignin-Chemistry, Structure, and Application. https://doi.org/10.5772/intechopen.106527
[16] Chen, F., Tobimatsu, Y., Jackson, L., Nakashima, J., Ralph, J., Dixon, R.A. (2013). Novel seed coat lignins in the Cactaceae: Structure, distribution and implications for the evolution of lignin diversity. The Plant Journal, 73: 201-211. https://doi.org/10.1111/tpj.12012
[17] Tobimatsu, Y., Chen, F., Nakashima, J., Jackson, L.A., Dixon, R.A., Ralph, J. (2013). Coexistence but independent biosynthesis of catechyl and guaiacyl/syringyl lignins polymers in seed coats. The Plant Cell, 25(7): 2587-600. https://doi.org/10.1105/tpc.113.113142
[18] Barsberg, S., Rasmussen, H.N., Kodahl, N. (2013). Composition of Cypripedium calceolus (Orchidaceae) seeds analyzed by attenuated total reflectance IR spectroscopy: In search of understanding longevity in the ground. American Journal of Botany, 100(10): 2066-2073. https://doi.org/10.3732/ajb.1200646
[19] Gamarra, R., Ortúñez, E., Cela, P.G., Merencio, A. (2018). Seed micromorphology of Orchidaceae in the Gulf of Guinea (West Tropical Africa). Plant Systematic and Evolution, 304: 665-677. https://doi.org/10.1007/s00606-018-1497-0
[20] Diantina, S., McCormick, A.C., Pritchard, H.W., Millner, J., Nadarajan, J., Mastur, M., McGill, C. (2022). Orchid seed micro-morphometry: Importance to species' biology, ecology, and conservation. In II International Symposium on Tropical and Subtropical Ornamentals, 1334: 153-162. https://doi.org/10.17660/ActaHortic.2022.1334.19
[21] Aprilianti, P., Handini, E., Puspitaningtyas, D.M. (2021). A seed morphometry study of selected species of Bulbophyllum and Dendrobium (Orchidaceae) in relation to their dispersals. Biodiversitas, 22(12): 5564-5571. https://doi.org/10.13057/biodiv/d221241
[22] Şeker, Ş.S., Akbulut, M.K., Şenel, G. (2021). Seed morphometry and ultrastructure studies on some Turkish orchids (Orchidaceae). Microscopy Research and Technique, 84(10): 2409-2420. https://doi.org/10.1002/jemt.23796
[23] GBIF Occurrence Download. GBIF. https://doi.org/10.15468/dl.6mpvve
[24] Popescu, M.C., Popescu, C.M., Lisa, G., Sakata, Y. (2011). Evaluation of morphological and chemical aspects of different wood species by spectroscopy and thermal methods. Journal of Molecular Structure, 988(1-3): 65-72. https://doi.org/10.1016/j.molstruc.2010.12.004
[25] Coates, J. (2000). Interpretation of infrared spectra, a practical approach. Encyclopedia of Analytical Chemistry, 12: 10815-10837.
[26] Nandiyanto, A.B.D., Oktiani, R., Ragadhita, R. (2019). How to read and interpret FTIR Spectroscopy of organic material. Indonesian Journal of Science & Technology, 4(1): 97-118. https://doi.org/10.17509/ijost.v4i1.15806
[27] Aytar, E.C., Durmaz, A., Basili, T., Senturk, B., Harzli, I., Cokmenz, B., Kompe, Y.O. (2024). Chemical characterization of the seed coats of orchids from the subfamily Orchidaceae: A micromorphological approach using FT-IR Spectroscopy. Biology Bulletin, 51(6): 1556-1567. https://doi.org/10.1134/S1062359024608498
[28] Salim, R.M., Asik, J., Sarjadi, M.S. (2021). Chemical functional groups of extractives, cellulose, and lignin extracted from native *Leucaena leucophala* bark. Wood Science and Technology, 55: 295-313. https://doi.org/10.1007/s00226-020-01258-2
[29] Kendon, J.P., Rajaovelona, L., Sandford, H., Fang, R., Bell, J., Sarasan, V. (2017). Collecting near mature and immature orchid seeds for ex situ conservation: In vitro collecting as a case study. Botanical Studies, 58: 34. https://doi.org/10.1186/s40529-017-0187-5
[30] Puspitaningtyas, D.M., Handini, E. (2020). Ex-situ conservation of Cymbidium finlaysonianum by seed storage. Biodiversitas, 21(8): 3519-3524. https://doi.org/10.13057/biodiv/d210813
[31] Ortunez, E., Perez-Guillen, A., Gamarra, R. (2025). Characterization of fruit and seed development in the genera Anacamptis and Serapias (Orchidaceae). Plants, 14(8): 1229. https://doi.org/10.3390/plants14081229
[32] Yan, X.N., Tian, M., Liu, F., Wang, C.X., Zhang, Y. (2017). Hormonal and morphological changes during seed development of *Cypripedium japonicum*. Protoplasma, 254: 2315-2322. https://doi.org/10.1007/s00709-017-1128-6
[33] Augustine, J., Yogendrakumar, K., Sharma, J. (2001). Orchids of India-II. Biodiversity status of *Bulbophyllum* Thou. Daya Publishing House, New Delhi, p.158. https://www.nhbs.com/orchids-of-india-volume-2-book.
[34] Hariyanto, S. (2019). Variations in seed micromorphology and morphometry of native Indonesian Phalaenopsis and Paphiopedilum orchids. Biodiversitas, 20(12): 3559-3567. https://doi.org/10.13057/biodiv/d201214
[35] Chaudhary, B., Chattopdhyay, P., Banerjee, N. (2014). Modulations in seed micromorphology reveal signature of adaptive species-diversification in Dendrobium (Orchidaceae). Open Journal of Ecology, 4(2): 33-42. https://doi.org/10.4236/oje.2014.42005
[36] Swamy, K.K., Krishna Kumar, H.N., Ramakrishna, T.M., Ramaswamy, S.N. (2004). Studies on seed morphometry of epiphytic orchids from Western Ghats of Karnataka. Taiwania, 49(2): 124-140.
[37] Pierce, S., Spada, A., Caporali, E., Ceriani, R.M., Buffa, G. (2019). Enzymatic scarification of Anacamptis morio (Orchidaceae) seed facilitates lignin degradation, water uptake and germination. Plant Biology, 21(3): 409-414. https://doi.org/10.1111/plb.12694
[38] Zhang, Y.Y., Wu, K.L., Zhang, J.X., et al. (2015). Embryo development in association with asymbiotic seed germination in vitro of Paphiopedilum armeniacum

S.C. Chen et F.Y. Liu. Scientific Reports, 5: 16356. https://doi.org/10.1038/srep16356

[39] Wagner, A., Tobimatsu, Y., Phillips, L., Flint, H., Torr, K., Donaldson, L., Pears, L., Ralph, J. (2011). CCoAOMT suppression modifies lignin composition in *Pinus radiata*. The Plant Journal, 67(1): 119-129. https://doi.org/10.1111/j.1365-313x.2011.04580.x

[40] Xia, W.Y., Cui, C.D., Shao, L.P., et al. (2025). Efficient separation of catechyl lignin from castor seed coats via molten salt hydrate. Separation and Purification Technology, 353: 128487. https://doi.org/10.1016/j.seppur.2024.128487

[41] Zhuo, C.L., Rao, X.L., Azad, R., et al. (2019). Enzymatic basis for C-lignin monomer biosynthesis in the seed coat of *Cleome hassleriana*. The Plant Journal, 99(3): 506-520.

[42] Ristanti, E.Y. (2023). Catechyl-lignin tissues in Vanilla orchid and candlenut: Structure/property studies. Doctoral Dissertation, Virginia Polytechnic Institute and State University, Blacksburg, Virginia, USA. https://vtechworks.lib.vt.edu/items/8da93058-fecf-48d9-8470-91588de6b922.